Medical Engineering & Physics 33 (2011) 374–380

Contents lists available at ScienceDirect

Medical Engineering & Physics

journal homepage: www.elsevier.com/locate/medengphy

Balancing incompatible endoprosthetic design goals: A combined ingrowth and bone remodeling simulation

M. Tarala[a,*], D. Janssen[a], N. Verdonschot[a,b]

[a] Orthopaedic Research Laboratory, Radboud University Nijmegen Medical Centre, Nijmegen, The Netherlands
[b] Laboratory for Biomechanical Engineering, University of Twente, Enschede, The Netherlands

ARTICLE INFO

Article history:
Received 25 February 2010
Received in revised form 5 November 2010
Accepted 7 November 2010

Keywords:
Cementless implant
Micromotions
Ingrowth
Bone remodeling

ABSTRACT

In order to design a good cementless femoral implant many requirements need to be fulfilled. For instance, the range of micromotions at the bone–implant interface should not exceed a certain threshold and a good ratio between implant–bone stiffness that does not cause bone resorption, needs to be ensured. Stiff implants are known to evoke lower interface micromotions but at the same time they may cause extensive resorption of the surrounding bone. Composite stems with reduced stiffness give good remodeling results but implant flexibility is likely to evoke high micromotions proximally. Finding a good balance between these incompatible design goals is very challenging. The current study proposes a finite element methodology that employs subsequent ingrowth and remodeling simulations and can be of assistance when designing new implants. The results of our simulations for the Epoch stem were in a good agreement with the clinical data. The proposed implant design made of porous tantalum with an inner CoCrMo core performed slightly better with respect to the Epoch stem and considerably better with respect to a Ti alloy stem. Our combined ingrowth and remodeling simulation can be a useful tool when designing a new implant that well balances mentioned incompatible design goals.

1. Introduction

Survival of cementless implants depends on growth of bone into and onto the implant surface. To facilitate bone ingrowth, micromotions at the implant–bone interface should be minimized as these may lead to implant loosening [1]. Therefore, in order to ensure an acceptable range of implant–bone motion, high-stiffness materials are used for prosthetic components. However, these components can drastically change the bone stress distribution with respect to the preoperative situation. After total hip arthroplasty (THA), loads that were originally transferred through bone are carried mainly by the prosthetic component, which results in stress shielding and subsequent bone remodeling around the implant. The stiffness mismatch between the bone and the femoral implant may cause bone resorption [2,3], subsequently leading to weakening of the complete reconstruction. Therefore, to reduce peri-prosthetic stress shielding, implants with a generally low bending stiffness could be an option. Hence, on the one hand high-stiffness implants reduce micromotions, while on the other hand low-stiffness implants reduce peri-prosthetic bone remodeling.

In order to optimize a cementless implant, a balance has to be found between these two incompatible design goals [4]. To screen the potential effects of composition changes of a femoral stem on bone, finite element (FE) models can be used. One can create a case-specific validated model [5,6] and simulate the outcome of various physiological processes like bone osseointegration [7] or bone remodeling [8]. To find a balance between these incompatible design goals one needs to investigate micromotions at the implant–bone interface as commonly done in many FE studies [9,10] but also look at bone remodeling.

In the present study we propose an FE methodology that combines an ingrowth and remodeling simulation. This method can be of assistance when designing new prosthetic components. To our knowledge there are only two FE studies (from one group of authors) where such an approach has been employed [7,11]. In the study of Fernandes et al. [11] bone ingrowth was simulated when the relative displacement at the interface was less than a threshold value. In such a case the initial frictional interface was bonded. Simultaneously, peri-prosthetic bone remodeling was simulated. In the current study, we propose a different approach where we first simulate the early stage ingrowth process to establish an equilibrium interface condition. This interface condition is subsequently

* Corresponding author at: Radboud University Nijmegen Medical Centre, Orthopaedic Research Laboratory, P.O. Box 9101, 6500 HB Nijmegen, The Netherlands. Tel.: +31 24 36 17461; fax: +31 24 35 40555.
E-mail address: M.Tarala@orthop.umcn.nl (M. Tarala).

1350-4533/$ – see front matter © 2010 IPEM. Published by Elsevier Ltd. All rights reserved.
doi:10.1016/j.medengphy.2010.11.005

Table 1
Proposed stem compositions and their bending stiffness.

Name	Neck	Inner	Middle	Outer	Bending stiffness (10^3 Nm^2)
Epoch	CoCrMo	CoCrMo	PEEK	Fiber metal	116.7
Ti alloy	TiAlV	TiAlV	TiAlV	TiAlV	260.8
Ta60	CoCrMo	60% porosity Ta	60% porosity Ta	60% porosity Ta	14.4
Ta80	CoCrMo	80% porosity Ta	80% porosity Ta	80% porosity Ta	4.5
Ta80-solid core	CoCrMo	CoCrMo	80% porosity Ta	80% porosity Ta	107.9

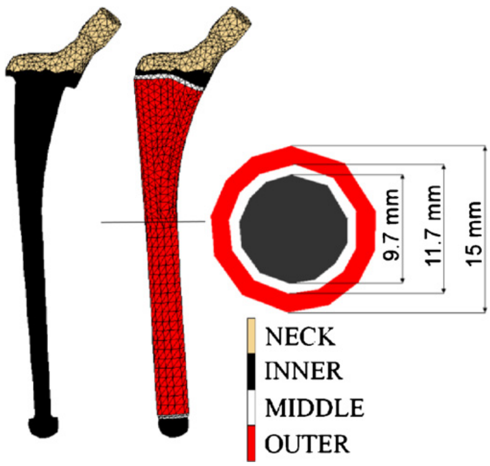

used in the remodeling simulation, which typically takes place the first few years after the operation.

We evaluated the use of porous tantalum to improve upon an already existing well-performing composite design using the FE method. As a well performing design we chose the VerSys Epoch FullCoat stem for its external surface characteristics and relatively low bending stiffness with respect to other designs [12,13]. Porous tantalum is a relatively new material and can be manufactured in a range of porosities with corresponding stiffness values. In addition, porous tantalum has a proven bone ingrowth capacity [14,15] thanks to its porosity and high frictional characteristics. These material properties have been utilized for various cup components [15], and there is one femoral stem design that utilizes Trabecular Metal material (Zimmer® Trabecular Metal™ Primary Hip Prosthesis).

In the present study we performed analyses to investigate the effects of various constitutions of tantalum material distributions on bone ingrowth. Subsequently we selected the three best performing designs and analyzed these in a bone remodeling simulation, to examine which implant design is best capable of balancing the two incompatible design goals. We addressed the question whether our methodology of subsequent ingrowth and remodeling simulation give a good insight when designing cementless femoral implants. We therefore applied this methodology to prosthetic designs containing various configurations of tantalum material.

2. Methods

Our case-specific FE model of bone was created from CT data of a human femur (81-year-old male, left femur). The bone was CT scanned along with a calibration phantom (solid, 0, 50, 100, 200 mg/ml calcium hydroxyapatite, Image Analysis, Columbia, KY, USA); subsequently the data was processed using a medical imaging software package (MIMICS 11.0). The model of the implant (VerSys Epoch FullCoat design (Zimmer, Inc., Warsaw, IN, USA)) was provided by the manufacturer and solid meshed using an FEA preprocessor (Marc 2007r1, MSC Software). All models were built from linear four-noded tetrahedral elements. The stem was positioned in the virtual bone by an experienced surgeon, using in-house software which allows the user to manipulate a solid model within the visualized CT-data (DCMTK MFC 10.8). We simulated the large amount of gaps (area of gaps of 21%) that are usually present at the bone–implant interface [16] using an in-house algorithm [17]. In order to create gaps at the interface an initial node-to-node surface mesh of bone and implant was created. Subsequently, the in-house algorithm was used to move the contour of intramedulary canal towards bony volume where local CT-values (Hounsfield Units, HU) were lower than a defined threshold. The isotropic properties of cortical and trabecular bone were derived from calibrated CT data. The calibration phantom was used to convert HU to calcium equivalent densities (ρ_{CHA}). An in-house software package was used to assign a calcium equivalent density (ρ_{CHA}) to each element, based on the average ρ_{CHA} value of all pixels in the element volume. The ash density was computed using relationships specific to the type of phantom used ($\rho_{ash} = 0.0633 + 0.887\rho_{CHA}$). The elastic modulus ($E$, MPa) was computed for each element from ash density (ρ_{ash}) using correlations for trabecular and cortical bone [18]. In the present study we used ash to apparent density ratio (ρ_{ash}/ρ_{app}) equal to 0.6 over the whole density range [19].

The Epoch stem is a layered composite construct consisting of a CoCrMo core, a PEEK inner layer and an outer Ti fiber metal layer. In order to analyze the various material combinations we kept the same layers but assigned them with different material properties (Table 1).

2.1. Ingrowth simulation

We first analyzed the effects of the varied composition on interfacial micromotions and bone ingrowth. Micromotions were defined as shear motion of implant nodes with respect to the local surface of the bone taking into account local deformation of the bone. Both the shear motion and gap opening were computed for each interface stem node. Bone osseointegration was assumed to occur when micromotions at the implant–bone interface remained below 40 μm [1] and the interfacial gap remained smaller than 500 μm [20] for 5 subsequent increments (Fig. 1). Though, this number does not represent real time period it gives an indication that the local conditions allowing for ingrowth were constant under varied loading configurations (unloaded–loaded, loaded–unloaded) for a defined time. Ingrowth was simulated by means of activating springs between a stem node and its adjacent bone node. The stiffness of a spring could be changed at any time (spring activation = ingrowth). The spring constant was defined tak-

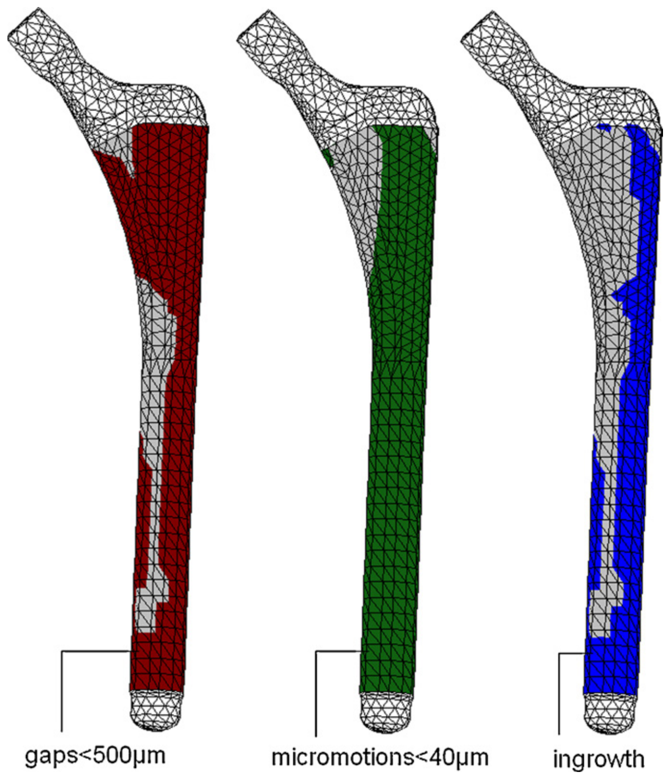

Fig. 1. Distribution of factors (gaps and micromotions) that govern the ingrowth process (Ta80). Note that ingrowth can be also jeopardize by high local bone stresses (proximally for the current figure).

ing into account the local bone material properties. We assumed the newly created bone had mechanical properties similar to that of the surrounding bone since the ingrowth and shear strength of the interface is greater in the cortical region [20,21]. The spring constant was therefore defined as the summation of the adjacent bone elements' Young's Modulus multiplied by 1/3 of the corresponding element face area (each face had 3 nodes connected to it), divided by the original spring length (equal to the gap between implant and bone node). In some cases, activating a spring locally caused excessive stresses at the implant–bone interface. If the local bone stresses exceeded 25 MPa, the springs were deactivated again, assuming failure of the bond. Reconstructions were subjected to normal walking loading conditions [22]. As potential implant compositions, we chose porous tantalum (Ta) in three constitutions: Ta60, Ta80 and Ta80-solid core (Table 1). The Ta60 and Ta80 compositions were built of porous tantalum with corresponding porosities (60% and 80%), while the implant neck was made of CoCrMo alloy. The Ta80-solid core composition consisted of a CoCrMo alloy core surrounded by a layer of porous tantalum (80% porosity). In addition, as reference stems we used the Epoch stem (existing design) and a solid Ti alloy stem with the grid blasted surface finish (hypothetical design, used to allow comparison to a commonly utilized construct). For each material corresponding material properties and frictional characteristics were applied (Table 2).

2.2. Bone remodeling simulation

Secondly, the three best-performing reconstructions (area of bone ingrowth) as predicted by the bone ingrowth simulations were analyzed in a bone remodeling simulation. We used strain adaptive remodeling theory to simulate changes in bone mineral density in time ($d\rho/dt$) [23]. The difference in local strain energy density per unit of bone mass between the preoperative (R_{ref}) and postoperative situation was taken as a stimulus (S) for bone remodeling when outside a dead zone ($((1-D)\times R_{ref})/((1+D)\times R_{ref})$, D-dead zone value). When S falls within the dead zone, no remodeling is assumed to occur ($d\rho/dt=0$). When S is smaller or greater than the dead zone, bone resorption or apposition will take place, respectively. In the current model the remodeling signal was averaged over the three following loading conditions ($S=(S_1+S_2+S_3)/3$). The reconstructions were subjected to an alternating loading history of normal walking and stair climbing. The normal walking consisted of two peak hip joint forces occurring during the walking cycle (the beginning and end of single support phase). The stair climbing load consisted of the peak force occurring during a stair climbing cycle. The local rate of mass change was also dependent on the density, based on the assumption that the remodeling rate depends on the size of the available free bone surface. Typically, the free surface is low in case of low bone density and in case of very high density [24]. Time in the remodeling simulation (computer time unit, ctu) depends on the maximum stimulus per iteration, the greater the stimulus the smaller the time iteration. Our FE remodeling prediction was fitted to clinical data [25] on the Epoch design to define the adequate 'dead zone' value and to allow for scaling of the time unit in the bone remodeling simulation. The clinical data used for the correlation existed of a 2 year clinical follow-up study by Akhavan et al. of the Epoch stem, in which the bone mineral density was monitored [25] (Fig. 2). The best fit was obtained for dead zone value 0.35 and time unit 60 (meaning that 60 ctu correspond to 2 year clinical reality) (Fig. 3). The implant–bone interface was assumed to be bonded only at locations where ingrowth was predicted in the previous simulations, with frictional contact in the remaining area. To allow for clinically relevant interpretation of the remodeling results, we used an in-house software package (DCMTK MFC 10.8) to project the results of the remodeling simulation onto 2D DEXA images. First, a 3D (X, Y, Z) voxel mesh is mapped onto the

Table 2
Material properties used in FE models.

Material	Young's modulus (GPa)	Poisson's ratio	Implant–bone friction coefficient
CoCrMo	240	0.3	n/a
PEEK	3.4	0.3	n/a
Fiber mesh	6.9	0.3	0.5 [44]
TiAlV	105	0.3	0.5 [45]
60% porosity Ta	5.8	0.34	0.88 [46]
80% porosity Ta	1.8	0.37	0.88 [46]

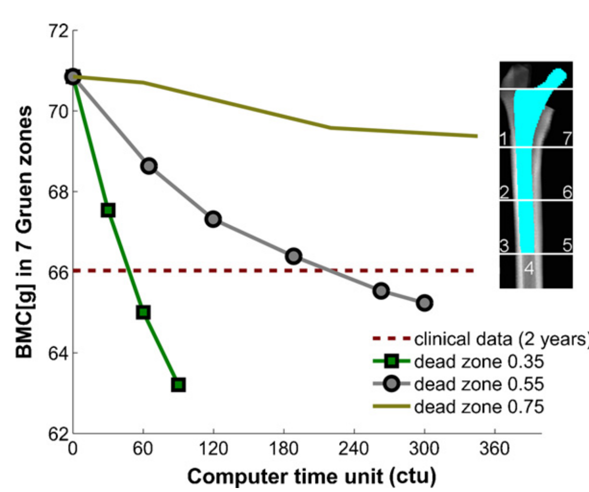

Fig. 2. Tuning of remodeling simulation with choice of three dead zones. Dead zones 0.35 and 0.55 gave good predition for the bone mineral content (BMC) within resonable time unit (ctu).

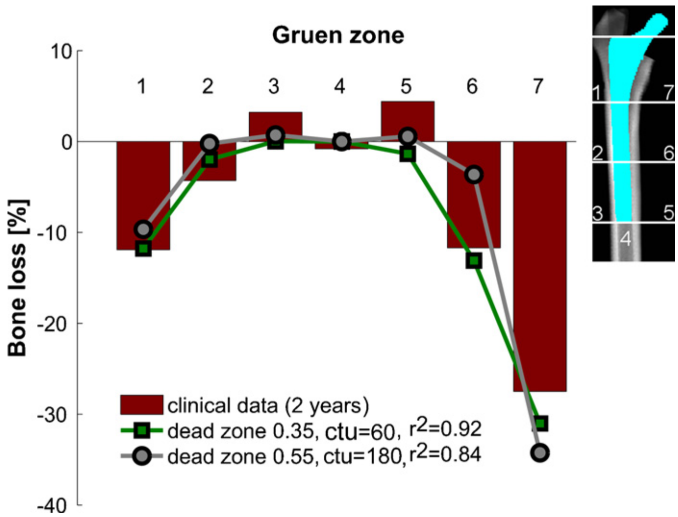

Fig. 3. Correlation results between the clinical (2 years in situ) data and data obtained from the remodeling simulations allowed us to define the best dead zone and real time.

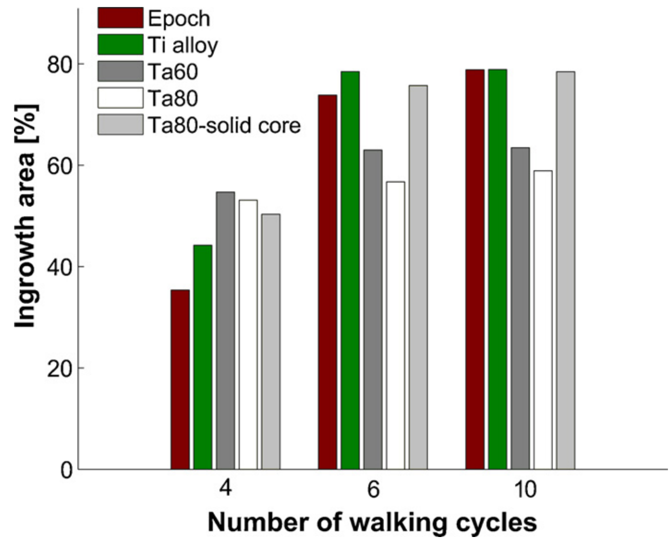

Fig. 5. Ingrowth area (%) for two standard designs (Epoch, Ti alloy) and three potential porous tantalum designs (Ta60, Ta80, Ta80-solid core).

FE reconstruction (Fig. 4). Subsequently, for each bone tetrahedral element its intersection volume with each voxels is calculated. The intersection volume is then multiplied by calcium equivalent of the element and added to the calcium equivalent of the corresponding voxels. Subsequently, a 2D pixel mesh with known calcium equivalent is created according to the chosen DEXA plane (e.g. (X, Y)). Each pixel has a calcium equivalent value corresponding to the summation of the values of 3D voxels (X_1, Y_1, $Z_{1/n}$) along the same (X_1, Y_1) coordinates. Non-bone elements do not contribute to the amount of calcium. In fact, if they were present along the (X_1, Y_1) coordinate when converting to the 2D pixel mesh, the pixel will be visualized as a stem pixel on the DEXA. We defined the seven Gruen zones [26] and computed bone density (g/cm^2) and local bone mineral content (BMC) (g) at different time points. We calculated bone density at each Gruen zone after one, two, three, four, five and ten years post-operatively for each implant composition. The bone loss predicted by our simulations was defined as a percentage of the pre-operative bone mass.

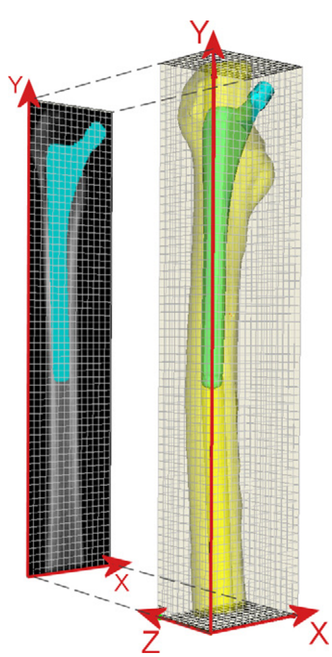

Fig. 4. An in-house software for converting numerical data.

3. Results

Of the proposed stem compositions three performed equally well in terms of predicted ingrowth. The Ti-alloy reached the ingrowth level of 80% the fastest, followed by the Ta80-solid core (which showed the highest ingrowth area of all after 4 cycles) and the Epoch (Fig. 5). The two stems composed only of porous tantalum (Ta60 and Ta80) achieved a similar ingrowth level (60% of the implant surface). Hence, the stems composed only of porous tantalum were too flexible, causing micromotions above 40 μm which occurred primarily at the proximal level.

Bone remodeling simulations were subsequently performed with the other 3 stem types (Epoch, Ti alloy and Ta80-solid core). The stem made of Ti alloy caused the greatest bone resorption in almost all Gruen zones. For all three designs the bone loss mainly occurred in the proximal part of the femur, with the greatest bone resorption in Gruen zone 7 (up to 75% after 10 year for Ti alloy stem). There was only a small difference between the remodeling of the Epoch and Ta80-solid core reconstructions (Fig. 6). These implants caused minimal bone loss in the distal region and the greatest in Gruen zone 7. These findings are consistent with the clinical measurements reported by Akhavan et al. [25]. The Ta80-solid core reconstruction had the least bone loss, although the difference with the Epoch was marginal.

Quantitatively, the bone loss in the reconstruction with the Ti alloy stem was 23 g after 10 years. After 10 years the Ta80-solid core stem and the Epoch stem displayed a bone loss of 11 g and 12 g, respectively. The change in BMC stabilized in time, the greatest changes were predicted to occur during the first 5 years, for all the models (Fig. 7).

Besides the DEXA prediction of bone loss, we calculated the total BMC of the complete bone in time, including the regions obscured by the implant in the DEXA measurements. The overall change in BMC corresponded with the changes seen in the 7 Gruen zones. After 10 years, the total bone loss was equal to 36 g, 19 g and 16 g for the Ti alloy, Epoch and Ta80-solid core stems, respectively. Considering the differences in bone loss measured with the DEXA and computed for the complete bone, one can note that considerable change also occurred in the bone obscured by the stem on the DEXA scans.

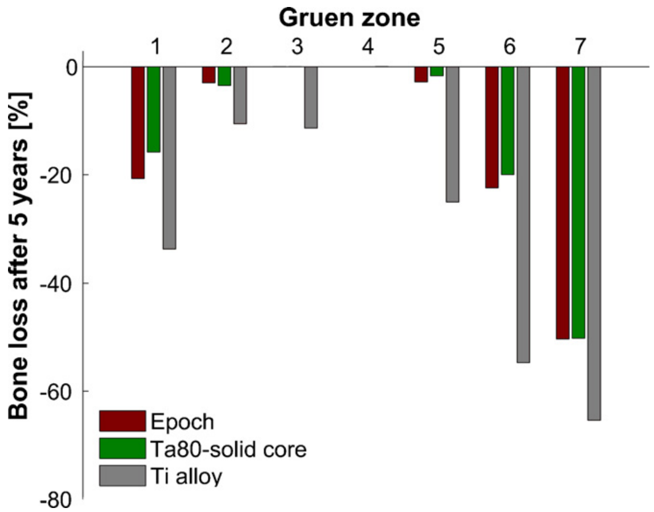

Fig. 6. Change in bone mineral content (BMC) predicted at 5 years by the FE remodeling simulation.

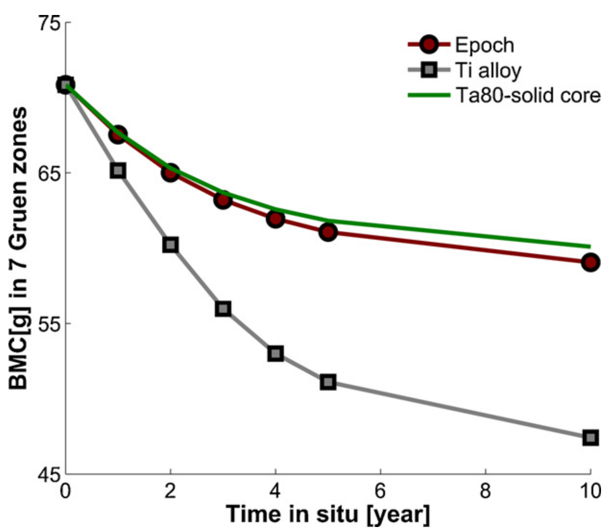

Fig. 7. Bone loss predicted by FE simulation at seven Gruen zones (1–7).

4. Discussion

In the present study by means of a combined design philosophy we attempted to improve upon the VerSys Epoch FullCoat stem using porous tantalum material. A common approach is to change implant composition and design so that micromotions and interface stresses are reduced and will allow bone ingrowth. Our in-house ingrowth simulation allowed us to follow the ingrowth process of different implant compositions. The osseointegration simulation showed its sensitivity to the different reconstructions. Initially there were considerable differences in the ingrowth process between designs. Tantalum design with a solid core performed the best initially, achieving maximum ingrowth as the Epoch and Ti-alloy design when the process stabilized. Tantalum designs without a solid metal core showed to be too flexible for successful fixation. This finding was consistent with the results already presented in literature [27] where high interface stresses occurred proximally for an iso-elastic stem. The Ta60 and Ta80 stems represented iso-elastic femoral implants since their material properties (1.8 GPa and 5.8 GPa) were in the lower range of bone stiffness.

This study adopts a combined FE approach to improve prosthetic design. We defined an ingrowth process based on acceptable ranges of micromotions and gaps for osseointegration. Our choice was supported by the outcome of clinical studies where thresholds for shear motion and gaps were defined for optimal bone ingrowth [1,20]. We recreated the actual interface gaps that represent the irregularity of the implant–bone interface making the ingrowth prediction more realistic. Furthermore, our remodeling simulation was successfully validated against clinical data which allowed us to select an optimal dead zone and subsequently correlate computer time units with real time. The changes in bone density predicted by our bone remodeling theory were quantitatively similar to the clinical data with respect to the region of occurrence. In many previous studies, a converged state was taken as a final remodeling result [11] while another study shows that this state tends to overestimate bone remodeling of bone [28].

The remodeling simulations showed that the composite stems performed better than the stem made of solid Ti alloy. This finding was consistent with the results of Turner et al. [29], where a decrease of bone mineral density around the Epoch stem was half of that surrounding the titanium alloy stem in Gruen zone 7. Our combined FE approach indicates that, from a theoretical point of view, the Epoch design and Ta80-solid core stem are best suitable to balance the incompatible design goals for cementless femoral implants.

A limitation to our study was that the ingrowth and remodeling analyses were separated, while *in vivo* there may actually be an overlap of the two processes. We based our assumption on previous studies on bone ingrowth and remodeling. Ingrowth occurs directly after implantation if the local conditions allow it (acceptable range of micromotions [1,30], no infection [31]). For instance, porous tantalum achieves an almost complete incorporation within 16 weeks, with little change after 1 year [14]. Bone remodeling, however, is a more long term process, although density changes already take place during the first few months after operation. Bodén et al. [32] reported that the decrease in bone mineral density (BMD) continued after 2 years and in Gruen zone 7 it was faster than the rate of bone loss on the control side. Also Mueller et al. [33] reported decrease in trabecular and cortical bone density especially in the calcar region between the 1 and 6 year examinations. Although these studies indicate there are differences between the stages during which ingrowth and remodeling takes place, currently there is no data available that would allow for a reliable determination of the relative timeframes.

Limitations of this study are also related to the bone remodeling theory and FE modeling. The remodeling rule is limited to the internal remodeling and no correction for geometrical changes was made. Additionally, our study was limited to only one implant shape, while other prosthetic designs may display greater sensitivity to the optimization process with porous tantalum material. The outcome of our study was also bone-quality dependent. An inverse relationship has earlier been reported between decrease of bone mineral content of an implanted femur with the bone mineral content of the contralateral control femora [34]. The results could be different when e.g. an osteoporotic bone or a prosthesis with a different fit (proximal vs. distal) were chosen.

The main limitation of our osseointegration simulation was the assumptions made for the ingrowth process. Ingrowth factors were identical for all stem compositions, whereas these may be more favorable for porous tantalum relative to the fiber mesh of the Epoch stem or grit-blasted Ti alloy stem. For instance, the differences in porosity of various coatings result in weaker or stronger bone apposition and interface shear strength [35,36] but this factor was not implemented in our simulation. On the other hand, our assumption might be considered necessary in order to be able to compare and choose the best performing design. In spite of the assumptions made, the ingrowth area predicted for the Epoch reconstruction was corresponding with the clinical data [25] where

73.57% (±8.48) along the entire length of the stem showed bone ingrowth after 48 months in situ. One can speculate that tantalum implants may have a higher ingrowth potential than predicted by our simulations [14,15].

Furthermore, it needs to be mentioned that we analyzed only one case-specific model, based on a single CT-scan and on one implant design. Although the selected femur was considered to be average in terms of shape, size and bone mineral density, the current results are influenced by the bone quality and implant position in the intramedulary canal.

In addition, we chose a specific stem design for our analyses. Evidently, the type of stem analyzed in this study is different from regular stem designs that are being used more frequently. Due to the low structural stiffness, one would expect to find micromotions higher than those found in regular stems. However, as the study of Kärrholm et al. [37] suggests, the subsidence of the Epoch stem is similar to that of a stiffer implant, which would disqualify the theoretical risk of increased interfacial micromotions. In the current study, we also included a stiff titanium alloy design, based on the Epoch shape. Our results indicate that the micromotions of the 'stiff' Epoch and the original isoelastic Epoch stem are very similar. Additionally, also in the study of Kärrholm et al. a stiffer design was associated with more proximal bone loss than the Epoch stem. Although this does not provide a direct proof, it gives an indication of the validity of our results and their applicability to other straight stem designs.

We performed subsequent ingrowth and remodeling simulations which could be argued a simplification of reality since the processes occur simultaneously. However, the relative relationship between the processes is not known sufficiently to allow reliable predictions by FE models. Since we separated the two processes and the interface conditions of the ingrowth simulation are implemented as an input of the remodeling process, the implant–bone interface will remain constant in the second simulation. Even high stresses occurred at the interface, the behavior between bone and implant will not be changed from bonded to frictional.

In conclusion, based on the results of this study we believe that a micromotion analysis in itself may not be sufficient to predict implant primary stability as commonly done in *in vitro* [38–40] and FE studies [10,41]. As shown in previous studies [42,43] and confirmed in the current, stiffer implants (e.g. Ti alloy stem) increase the interface stability and therefore give good results in ingrowth simulations. However, due to a discrepancy in bone and implant stiffness, our results indicate such implants have the potential to increase bone resorption compared to more flexible composite stems. We showed that to be able to judge implant stability one should perform an interfacial micromotions prediction study followed by a remodeling simulation. The methodology proposed in the present study can be a useful tool when designing a new implant or improving upon existing designs.

Acknowledgement

This study was funded in part by Zimmer, Inc., Warsaw, IN, USA.

Conflict of interest statement

We do not have any financial and personal relationships with other people or organization.

References

[1] Jasty M, Bragdon C, Burke D, O'Connor D, Lowenstein J, Harris WH. In vivo skeletal responses to porous-surfaced implants subjected to small induced motions. J Bone Joint Surg Am 1997;79(5):707–14.
[2] Huiskes R, Weinans H, Van RB. The relationship between stress shielding and bone resorption around total hip stems and the effects of flexible materials. Clin Orthop Relat Res 1992;(274):124–34.
[3] Head WC, Bauk DJ, Emerson Jr RH. Titanium as the material of choice for cementless femoral components in total hip arthroplasty. Clin Orthop Relat Res 1995;(311):85–90.
[4] Huiskes R. Failed innovation in total hip replacement. Diagnosis and proposals for a cure. Acta Orthop Scand 1993;64(6):699–716.
[5] Taddei F, Pancanti A, Viceconti M. An improved method for the automatic mapping of computed tomography numbers onto finite element models. Med Eng Phys 2004;26(1):61–9.
[6] Trabelsi N, Yosibash Z, Milgrom C. Validation of subject-specific automated p-FE analysis of the proximal femur. J Biomech 2009;42(3):234–41.
[7] Folgado J, Fernandes PR, Jacobs CR, Pellegrini Jr VD. Influence of femoral stem geometry, material and extent of porous coating on bone ingrowth and atrophy in cementless total hip arthroplasty: an iterative finite element model. Comput Methods Biomech Biomed Eng 2009;12(2):135–45.
[8] Van Rietbergen B, Huiskes R, Weinans H, Sumner DR, Turner TM, Galante JO. ESB Research Award 1992. The mechanism of bone remodeling and resorption around press-fitted THA stems. J Biomech 1993;26(4–5):369–82.
[9] Reggiani B, Cristofolini L, Varini E, Viceconti M. Predicting the subject-specific primary stability of cementless implants during pre-operative planning: preliminary validation of subject-specific finite-element models. J Biomech 2007;40(11):2552–8.
[10] Viceconti M, Brusi G, Pancanti A, Cristofolini L. Primary stability of an anatomical cementless hip stem: a statistical analysis. J Biomech 2006;39(7):1169–79.
[11] Fernandes PR, Folgado J, Jacobs C, Pellegrini V. A contact model with ingrowth control for bone remodelling around cementless stems. J Biomech 2002;35(2):167–76.
[12] Glassman AH, Crowninshield RD, Schenck R, Herberts P. A low stiffness composite biologically fixed prosthesis. Clin Orthop Relat Res 2001;(393):128–36.
[13] Hartzband MA, Glassman AH, Goldberg VM, Jordan LR, Crowninshield RD, Fricka KB, et al. Survivorship of a Low-stiffness extensively porous-coated femoral stem at 10 years. Clin Orthop Relat Res 2010;468(2):433–40.
[14] Bobyn JD, Stackpool GJ, Hacking SA, Tanzer M, Krygier JJ. Characteristics of bone ingrowth and interface mechanics of a new porous tantalum biomaterial. J Bone Joint Surg Br 1999;81(5):907–14.
[15] Levine BR, Sporer S, Poggie RA, la Valle CJ, Jacobs JJ. Experimental and clinical performance of porous tantalum in orthopedic surgery. Biomaterials 2006;27(27):4671–81.
[16] Prymka M, Wu L, Hahne HJ, Koebke J, Hassenpflug J. The dimensional accuracy for preparation of the femoral cavity in HIP arthroplasty. A comparison between manual- and robot-assisted implantation of hip endoprosthesis stems in cadaver femurs. Arch Orthop Trauma Surg 2006;126(1):36–44.
[17] Waanders D, Janssen D, Miller MA, Mann KA, Verdonschot N. Fatigue creep damage at the cement–bone interface: an experimental and a micro-mechanical finite element study. J Biomech 2009;42(15):2513–9.
[18] Keyak JH, Falkinstein Y. Comparison of in situ and in vitro CT scan-based finite element model predictions of proximal femoral fracture load. Med Eng Phys 2003;25(9):781–7.
[19] Schileo E, Dall'ara E, Taddei F, Malandrino A, Schotkamp T, Baleani M, et al. An accurate estimation of bone density improves the accuracy of subject-specific finite element models. J Biomech 2008;41(11):2483–91.
[20] Sandborn PM, Cook SD, Spires WP, Kester MA. Tissue response to porous-coated implants lacking initial bone apposition. J Arthroplasty 1988;3(4): 337–46.
[21] Clemow AJ, Weinstein AM, Klawitter JJ, Koeneman J, Anderson J. Interface mechanics of porous titanium implants. J Biomed Mater Res 1981;15(1):73–82.
[22] Heller MO, Bergmann G, Deuretzbacher G, Dürselen L, Pohl M, Claes L, et al. Musculo-skeletal loading conditions at the hip during walking and stair climbing. J Biomech 2001;34(7):883–93.
[23] Huiskes R, Weinans H, Grootenboer HJ, Dalstra M, Fudala B, Slooff TJ. Adaptive bone-remodeling theory applied to prosthetic-design analysis. J Biomech 1987;20(11–12):1135–50.
[24] Martin RB. Porosity and specific surface of bone. Crit Rev Biomed Eng 1984;10(3):179–222.
[25] Akhavan S, Matthiesen MM, Schulte L, Penoyar T, Kraay MJ, Rimnac CM, et al. Clinical and histologic results related to a low-modulus composite total hip replacement stem. J Bone Joint Surg Am 2006;88(6):1308–14.
[26] Gruen TA, McNeice GM, Amstutz HC. "Modes of failure" of cemented stem-type femoral components: a radiographic analysis of loosening. Clin Orthop Relat Res 1979;(141):17–27.
[27] Weinans H, Huiskes R, Grootenboer HJ. Effects of material properties of femoral hip components on bone remodeling. J Orthop Res 1992;10(6):845–53.
[28] Kerner J, Huiskes R, van Lenthe GH, Weinans H, Van RB, Engh CA, et al. Correlation between pre-operative periprosthetic bone density and post-operative bone loss in THA can be explained by strain-adaptive remodelling. J Biomech 1999;32(7):695–703.
[29] Turner AW, Gillies RM, Sekel R, Morris P, Bruce W, Walsh WR. Computational bone remodelling simulations and comparisons with DEXA results. J Orthop Res 2005;23(4):705–12.
[30] Pilliar RM, Lee JM, Maniatopoulos C. Observations on the effect of movement on bone ingrowth into porous-surfaced implants. Clin Orthop Relat Res 1986;(208):108–13.
[31] Cameron HU, Yoneda BT, Pilliar RM, Macnab I. The effect of early infection on bone ingrowth into porous metal implants. Acta Orthop Belg 1977;43(1):71–4.

[32] Bodén HS, Sköldenberg OG, Salemyr MO, Lundberg HJ, Adolphson PY. Continuous bone loss around a tapered uncemented femoral stem: a long-term evaluation with DEXA. Acta Orthop 2006;77(6):877–85.
[33] Mueller LA, Nowak TE, Haeberle L, Mueller LP, Kress A, Voelk M, et al. Progressive femoral cortical and cancellous bone density loss after uncemented tapered-design stem fixation. Acta Orthop 2010;81(2):171–7.
[34] Engh CA, McGovern TF, Bobyn JD, Harris WH. A quantitative evaluation of periprosthetic bone-remodeling after cementless total hip arthroplasty. J Bone Joint Surg Am 1992;74(7):1009–20.
[35] Friedman RJ, An YH, Ming J, Draughn RA, Bauer TW. Influence of biomaterial surface texture on bone ingrowth in the rabbit femur. J Orthop Res 1996;14(3):455–64.
[36] Kienapfel H, Sprey C, Wilke A, Griss P. Implant fixation by bone ingrowth. J Arthroplasty 1999;14(3):355–68.
[37] Kärrholm J, Anderberg C, Snorrason F, Thanner J, Langeland N, Malchau H, et al. Evaluation of a femoral stem with reduced stiffness. A randomized study with use of radiostereometry and bone densitometry. J Bone Joint Surg Am A 2002;84(9):1651–8.
[38] Schneider E, Kinast C, Eulenberger J, Wyder D, Eskilsson G, Perren SM. A comparative study of the initial stability of cementless hip prostheses. Clin Orthop Relat Res 1989;(248):200–9.
[39] Götze C, Steens W, Vieth V, Poremba C, Claes L, Steinbeck J. Primary stability in cementless femoral stems: custom-made versus conventional femoral prosthesis. Clin Biomech (Bristol, Avon) 2002;17(4):267–73.
[40] Bühler DW, Berlemann U, Lippuner K, Jaeger P, Nolte LP. Three-dimensional primary stability of cementless femoral stems. Clin Biomech (Bristol, Avon) 1997;12(2):75–86.
[41] Pancanti A, Bernakiewicz M, Viceconti M. The primary stability of a cementless stem varies between subjects as much as between activities. J Biomech 2003;36(6):777–85.
[42] Kuiper JH, Huiskes R. Friction and stem stiffness affect dynamic interface motion in total hip replacement. J Orthop Res 1996;14(1):36–43.
[43] Harvey EJ, Bobyn JD, Tanzer M, Stackpool GJ, Krygier JJ, Hacking SA. Effect of flexibility of the femoral stem on bone-remodeling and fixation of the stem in a canine total hip arthroplasty model without cement. J Bone Joint Surg Am 1999;81(1):93–107.
[44] Rancourt D, Shirazi-Adl A, Drouin G, Paiement G. Friction properties of the interface between porous-surfaced metals and tibial cancellous bone. J Biomed Mater Res 1990;24(11):1503–19.
[45] Shirazi-Adl A, Dammak M, Paiement G. Experimental determination of friction characteristics at the trabecular bone/porous-coated metal interface in cementless implants. J Biomed Mater Res 1993;27(2):167–75.
[46] Zhang Y, Ahn PB, Fitzpatrick DC, Heiner AD, Poggie RA, Brown TD. Interfacial frictional behavior: cancellous bone, cortical bone, and a novel porous tantalum biomaterial. J Musculoskelet Res 1999;3(4):245–51.